Photochemical & Photobiological Sciences

PAPER

View Article Online
View Journal | View Issue

Cite this: *Photochem. Photobiol. Sci.*, 2019, **18**, 1963

Transmission of ultraviolet, visible and near-infrared solar radiation to plants within a seasonal snow pack†

T. Matthew Robson * and Pedro J. Aphalo

Sunlight is strongly attenuated by the snowpack, causing irradiance to decrease exponentially with depth. The strength of attenuation is wavelength dependent across the spectrum. Changes in received irradiance and its spectral composition are used by plants as cues for the timing of phenology, and it is known that at shallow depths in the snowpack there is sufficient light for plants to photosynthesize if conditions are otherwise favourable. The spectral composition of solar radiation under snow in the visible region was already determined in the 1970s using scanning spectroradiometers, but spectral attenuation within the ultraviolet region (UV-B 280–315 nm, UV-A 315–400 nm) has not been well characterised because it is difficult to measure. We measured vertical transects of spectral irradiance (290–900 nm) transmitted through a settled seasonal snowpack. The peak transmission of radiation was in the UV-A region in the upper centimetres of the snowpack and transmittance generally declined at longer wavelengths. Given the known action spectra of plant photoreceptors, these results illustrate the possibility that changing UV-A : visible and red : far-red radiation ratios under the snowpack may serve as spectral cues for plants; potentially priming plants for the less stable environment they experience following snowmelt. Array spectrometers open opportunities for rapid and continuous measurement of irradiance in challenging environments, *e.g.* beneath the snowpack, and capturing changing light conditions for plants. Future research is needed to couple the spectral transmittance of snowpacks differing in their longevity and crystal structure with measurements of the perception and response to radiation by plants under snow.

Received 28th April 2019,
Accepted 18th July 2019

DOI: 10.1039/c9pp00197b

rsc.li/pps

Introduction

The winter snowpack is usually considered to be beneficial to the plants it covers in cold climates because of its moderating effect on temperature and irradiance. The snowpack insulates the ground, buffering changes in air temperature and partially attenuating solar radiation through reflectance and scattering by snowflakes. The small portion of the incident solar radiation which is not reflected is absorbed by or transmitted through the snowpack. The transmitted radiation is available to snow algae and plants within the snowpack for photosynthesis and carries information to organisms about their environment.[1–3] There is a long history of research testing how deep in the snowpack both photosynthesis and signalling functions remain possible for plants and algae, *e.g.* ref. 4. Early in the 20th Century, pyrheliometers and photo-electric cells with wavelength-selective filters were used for these measurements, and later scanning spectroradiometers were placed in elaborately-constructed snow tunnels allowing the extinction coefficients for photosynthetically active radiation (PAR: 400–700 nm) to be calculated along with the transmission through snow of each region of solar radiation in the visible spectrum.[5–7] However, in part because of the practical difficulties that such studies present, our knowledge of the transmission through the snowpack of UV radiation comes from a small number of tests (*e.g.* ref. 8–11). Likewise, measurements are scarce of differences in attenuation by snow across the solar spectrum comparing ultraviolet (UV-B 280–320 nm, UV-A 320–400 nm), photosynthetically active radiation (PAR: 400–700 nm), and the red-to-far-red ratio (R : FR, 655–665/725–735 nm)[12] (Table S1†).

The transmission of light through a homogeneous medium usually follows the Beer–Lambert law of exponential decline with depth.[13] In snow, this relationship holds only approximately as snow is an agglomerate of ice crystals of different shapes surrounded by air spaces, that is to say, it is an heterogeneous medium.[10] Strong back-scattering from ice particles in the snowpack increases the proportion of radiation moving

Organismal and Evolutionary Biology (OEB), Viikki Plant Science Centre (ViPS), P.O. Box 65, Faculty of Biological and Environmental Science, 00014, University of Helsinki, Finland. E-mail: matthew.robson@helsinki.fi

†Electronic supplementary information (ESI) available. See DOI: 10.1039/c9pp00197b

through air spaces altering the rate of extinction of solar radiation with depth. This back-scattering can in particular cause unexpectedly high values of irradiance in the top centimetres beneath the snow surface, *e.g.* ref. 1 and 9. Several studies have found clean snow to transmit enough incident solar radiation for photosynthesis to occur at a depth of 30 cm at midday (reviewed by ref. 2). At high elevation in the Rocky Mountains, sufficient solar radiation to serve as a cue for seeds to germinate was detected at 500 nm wavelength at a maximum snow depth of 198 cm under the snowpack on March 20th; but its transmission to greater depth was considered likely when solar irradiance and snow density are high and albedo low.[7] Spectral transmission of blue (420–490 nm) and green (500–570 nm) light is greater than red or far-red (Table S1†), giving a possible explanation for the pigmentation of red algae which can utilise green light in photosynthesis.[1,6]

To better understand the spectral attenuation by snow of solar radiation in the PAR and UV regions, the irradiance transmitted through a seasonal winter snowpack was measured along a vertical transect down to 20–24 cm depth from the surface of the snowpack. These measurements were made with an array spectrometer in Helsinki during February 2018 and repeated at the same location during January 2019. This allowed us to test the capacity of the device to function at a low temperature (to −19 °C) and to compare the instantaneous spectral transmittance of the snowpack across the solar spectrum at high wavelength (<1 nm) resolution along the vertical transects.

Methods

Measurement of spectral irradiance across a gradient of snow depth

Spectral irradiance was measured along a vertical transect through the snowpack on 28-02-2018 and on 27-01-2019 in an open ploughed field at Viikki Fields, Helsinki (61.22684°N 25.01921°E, 8 m asl). The age, compaction and grain size of the snowpack has a large effect on its spectral transmittance and most research in the last 25 years has focussed on polar- or long-duration snowpacks (*e.g.* ref. 8 and 9). In contrast, the seasonal snowpacks (40 cm deep) we measured were comprised of recently-settled rounded-grains of snow with no crust. These were classed as dry snowpacks and relatively homogeneous with depth.[14] In 2018, the snowpack was comprised of snow which fell predominantly between 10-02-2018 and 15-02-2018, whereas in 2019 snow fell on the 09-01-2019 and 17-01-2019. During formation of the snowpack the temperature did not rise above freezing (Appendix 2, ESI:† solar angles and weather data). Spectral irradiance was recorded 30 cm above the snow, and level with the horizontal surface of the snowpack, and at approximately 2 cm intervals below the snow, down to 24 cm depth, which corresponded to a height of approximately 15–20 cm above the ground. The measurements were centred around solar noon on days when the sky was completely clear; on 28-02-2018 from 13 : 20–14 : 20 EET (Eastern European Standard Time), solar elevation angle from 21.9°–18.8° and air temperature stable at about −13 to −15 °C (Appendix 2, ESI†), ozone column thickness 492 DU (Total Ozone Mapping Spectrometer, NASA, USA); on 27-01-2019, 12 : 05–13 : 45 EET, solar elevation angle from 11.5–10.9°, stable air temperature about −17 to −19 °C and ozone column thickness 395 DU (Appendix 2, ESI†). All equipment was placed *in situ* at the measurement location for about 20 min prior to the recordings to allow the temperature of the device to approach the ambient temperature.

Recordings of spectral irradiance were made using an array spectrometer, factory tuned for low stray light and maximum sensitivity in the UV region (Maya 2000 Pro, configured with a "short" 10 μm slit type 10s and #HC21 grating, Hamamatsu S10420 Back-thinned, 2DFFT-CCD detector with 200 nm OFLV filter; Ocean Optics, Dunedin, FL, USA), attached *via* a 2 m long optical fibre (OBIF600-UV-BX, Ocean Optics) to a circular cosine diffuser (45 mm diameter; DH-7, Bentham Instruments Ltd. Reading UK).[15] For measurements above the snowpack, the diffuser was levelled on a tripod in a sensor-holder incorporating a spirit level. On and below the surface of the snowpack, only the diffuser was in direct contact with the snow (Fig. S1†). A pit in the snowpack was made and for measurements at each depth the diffuser was inserted from the north side into the wall of the very loose snowpack at least 30 cm horizontally. Care was taken to disturb the structure of the snow as little as possible, and any snow which was disturbed to allow insertion of the diffusor was replaced by backfilling with loose snow before each measurement, as was the snow in the snow pit. Snow depth was measured with a ruler and tape measure.

The integration time used for recording for each measurement was set manually in Spectral Suite software (Ocean Optics, Dunedin, FL, USA) to obtain as good a resolution as possible in the UV region while not exceeding the maximum counts (60 000 counts) in the visible region. The average of two spectra was recorded at each depth, and bracketing employed to obtain high resolution spectra in the UV region in the upper 12 cm of the snowpack. Bracketing involved measuring a spectrum in just the UV region (<400 nm) at high resolution (integration time up to 8 s) and combining this with the entire spectrum (290–900 nm). At depths of greater than 14 cm deep in the snow pack, the maximum integration time (8 s) for the device was used for the entire spectrum so bracketing was not feasible. At and below 14 cm depth, readings in the UV-B region were very low and can not be considered reliable because of a low signal-to-noise ratio. These UV-B data are excluded from the analyses but remain plotted in the figures to illustrate the high noise and lack of precision in the UV-B region at very low irradiances.

A measurement with the diffusor covered by a darkening cap was used to correct for dark-noise at each integration time used, and for measurements above the snowpack an additional calibration with a UV-filter was employed to account for stray light in the UV region (<400 nm).[16] Spectra were pre-processed using the R packages ooacquire and photo-

biology[17] in R version 3.4.3 (R Core Team, 2018). Both processed and raw spectra were individually inspected at each 0.46 nm wavelength step and values from unresponsive pixels or dropping below zero in the UV-B region were discarded (no more than 10 per spectrum). A measured spectrum was compared with modelled spectra for the same hour of the same day (Fig. S2†), generated using *libRadtran* a library of radiative transfer protocols[18] as described in ref. 19.

To facilitate comparisons of spectral irradiance, irradiance was divided into spectral integrals (UV-B, UV-A, blue, green, R : FR *etc.*) and the extinction coefficients of irradiance with depth through the snowpack were fitted through regression for these regions with the function, eqn (1):

$$y = ae^{-bx} \quad (1)$$

Extinction coefficients were calculated for the upper 5 cm depth and down to 20 cm depth where: x is depth, a is the surface irradiance and b is the extinction coefficient in units of μmol m^{-2} s^{-1} cm^{-1}.

Results

Spectral irradiance decreased exponentially with depth through the snowpack across the regions of the spectrum captured by our spectrometer (Fig. 1, 290–900 nm), with 10% of the incident irradiance at the surface of the snowpack reaching 7 cm below the surface in both years. Low irradiances produced a low signal-to-noise ratio for UV-B at >12 cm depth and UV-A >16 cm depth, reducing our confidence in these data to a level where we omitted them from our calculations of extinction coefficients (Table 1). While the general trends were similar between transects measured on the two measurement dates, these trends differed in their magnitude and in some fine spectral features. The lower solar elevation angle in January 2019 than February 2018 resulted in 28%-lower incident PAR (400–700 nm), and 39%-lower UV-B irradiance, at the surface of the snowpack. This may be partially responsible for the absence of prominent peaks in transmittance, particularly at shorter wavelengths in the 2019 measurements.

The effects of the snow pack on the spectral transmission of radiation are easier to visualise when the irradiance spectra are plotted as a proportion of the irradiance at the snow surface (Fig. 2). This plot shows that transmission of solar radiation by the snowpack was not uniform across the spectrum (Fig. 2 and S3†). The function, eqn (1), for exponential attenuation of irradiance with depth was a good fit to the data within the selected range for the spectral integrals across UV-B, UV-A, and PAR (Tables 1 and S2, Fig. S4†). Of the variation in transmitted irradiance across PAR region of the 2018 transect (Fig. 2A), the small peak at approximately 515 nm is the most interesting (0–5 cm depth: $b = -0.241$, $R^2 = 0.938$); since a peak in this region of the spectrum has also been reported in the past from measurements at a lower spectral resolution of 10–50 nm intervals with a scanning spectroradiometer (Table S1†).

Transmission of UV-A radiation relative to PAR was particularly enhanced at shallow depths in the upper few centimetres of the snowpack (Fig. 2, S4 and S5,† Table 1; at 4 cm depth 25% of UV-A, but only 15–20% of PAR, irradiance was transmitted in both transects), but surprisingly transmission did not gradually continue to increase into the UV-B region (Fig. 2). Consequently, a peak in transmitted UV-A irradiance at about 365 nm was recorded on 28-02-2018, and a less pronounced rise and decline at shorter wavelengths on 27-01-2019. The trend for faster extinction of longer PAR wavelengths (>600 nm) was consistent in both years (Fig. 1 and 3, Table 1: 10–15% of far-red reaching 4 cm depth). The R : FR ratio increased with depth as far-red radiation was attenuated by the snowpack more than red light (Fig. 3). Near infra-red radiation was most-steeply attenuated with depth in the snowpack when comparing the all regions of the spectrum that we measured (Tables 1 and S4;† only 12–16% transmitted at 4 cm depth).

Discussion

Spectral irradiance along a gradient of snow depth

The progressively-reduced transmission of radiation through the snowpack with increasing wavelength that we recorded is consistent with past reports of wavelength dependence of irradiance under snow in the red, far-red and near infra-red regions (*e.g.* ref. 10 and 20; although not always those of snow on sea ice, see ref. 21). Prior to the 1980s, there were several comprehensive field studies of the transmittance of snow in the visible and near-infra-red (NIR) regions, but only a couple of subsequent studies have considered visible and UV radiation at wavelengths as low as 350 nm (Table S1†). Of these, the most detailed survey of transmission of PAR and UV-A radiation through snow was performed in Antactica.[9] In this study, the transmission of solar radiation through the snowpack was measured down to 135 cm depth with a 3 nm resolution to 350 nm, and a peak in transmittance was identified at 390 nm. This represents a slightly longer wavelength than the peaks in transmittance that we obtained (at 365 nm on 28-02-2018 and at <340 nm on 27-01-2019), but typically published studies have found peak transmittance by snowpacks approaching the low-wavelength limits of the instruments they used (Table S1†). The extinction coefficient of radiation in the snowpack is the sum of absorbance and backscattering of radiation, and it is worth noting in this context that snow has a peak in albedo at 350–360 nm.[22] A physical explanation related to the scattering of UV radiation by ice crystals in the upper centimetres of the snowpack is the most likely explanation for the peaks in transmittance reported in the UV-A region. Snow grains have an asymmetrical shape and crystals increase in size and take on more similar properties to ice with length-of-time in the snowpack and repeated freeze–thaw cycles. The unusual scattering properties of snow crystals, emanating from their complex and heterogeneous structure, are difficult to model,[23,24] and might explain the differences in the wave-

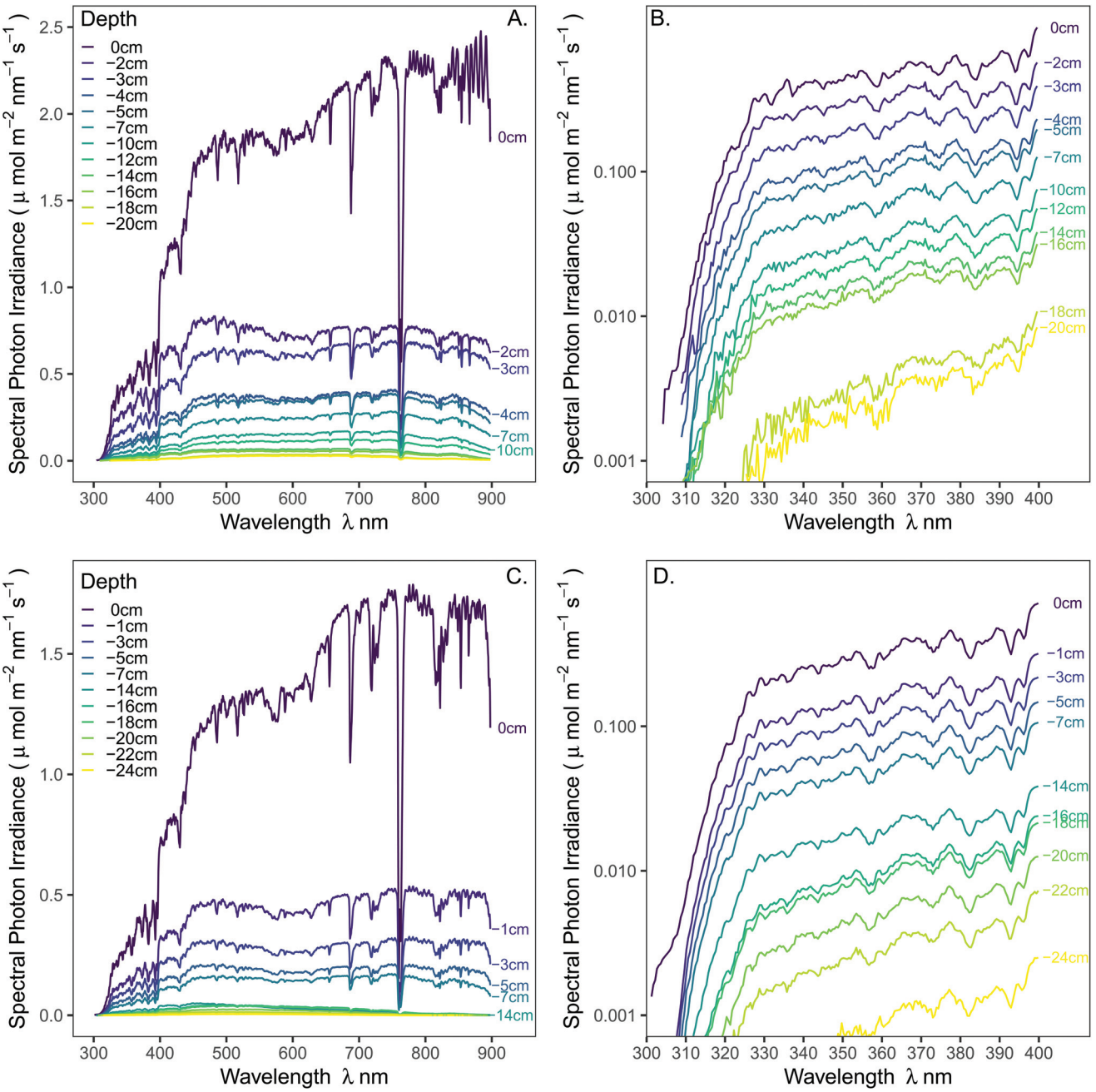

Fig. 1 Measured spectral irradiance on 28-02-2018 (A & B) and 27-01-2019 (C & D) at the snow surface (0 cm) and at depths beneath the snow surface creating a vertical transect presented on (A & C) a linear *y*-axis (full spectrum) and (B & D) a $\log_{10}$ axis (UV-region of the spectrum only).

lengths of maximum transmittance within the UV-A region between our two measurement dates.

Ray-tracing models of reflectance and transmittance through the snowpack suggest that, while differences in the crystal size and shape of grains of snow can affect the overall transmittance, they do not affect the spectral dependency of transmittance.[25] These models consistently give the highest albedo, lowest absorbance, and highest transmittance at the shortest modelled wavelength of 350 nm. However, the age, density and wetness of the snow can affect the spectral dependence of transmittance of measured irradiance with depth in old hard-packed snow compared with a seasonal snowpack.[8,10] Even so, the extinction coefficients that we obtained (Fig. S5† and Table 1) are in a similar range to these models[10] for the PAR region, and are consistent with those obtained in the majority of other field studies (Table S1†). Likewise, the trend for increased transmittance by the snowpack in the UV-A region compared with PAR is generally consistent across studies (Table S1†).

Table 1 Average spectral photon irradiance (μmol m^{-2} s^{-1}) given for spectral integrals, measured at 30 cm above the snow, at the snow surface (0 cm), and along a vertical transect beneath the snow surface down to 20 cm depth (28-02-2018). Ratios of certain spectral integrals are given: the UV-B : PAR ratio and the UV-B : UV-A ratio report UV-B × 1000 to give readable results. Each wavelength range and the R : FR ratio are defined by Sellaro.[12] The extinction coefficients of the fitted function to two alternative maximum depths are given. Table S2† gives these values for transects from 27-01-2019 which follow a similar trend to those presented here according to the extinction coefficients

Depth (cm)	PAR (PPFD)	UV-B	UV < 350 (nm)	UV > 350 (nm)	UV-A	Blue	Green	Red	Far-red	Infra-red (<900 nm)	UVB : UVA (×1000)	UVB : PAR (×1000)	UVA : PAR ratio	R : FR ratio	B : G ratio	B : R ratio
30 above	677.44	0.095	10.66	29.62	40.18	133.55	163.00	158.54	143.55	416.20	2.36	0.14	0.06	1.10	0.82	0.84
0	535.55	0.142	10.43	27.14	37.43	110.94	128.42	121.53	109.94	319.12	3.79	0.27	0.07	1.11	0.86	0.91
2	219.33	0.079	6.95	17.63	24.50	51.77	53.04	44.22	37.51	103.47	3.21	0.36	0.11	1.18	0.98	1.17
3	178.26	0.044	4.25	11.70	15.90	39.02	43.27	38.27	33.02	90.97	2.78	0.25	0.09	1.16	0.90	1.02
4	105.33	0.030	2.54	6.94	9.45	23.15	25.64	22.48	19.37	51.37	3.17	0.28	0.09	1.16	0.90	1.03
5	97.99	0.018	1.94	5.69	7.61	20.61	23.91	21.61	18.53	46.23	2.37	0.18	0.08	1.17	0.86	0.95
7	68.78	0.013	1.18	3.57	4.74	13.91	16.79	15.60	13.54	33.06	2.68	0.18	0.07	1.15	0.83	0.89
10	42.52	0.007	0.66	2.09	2.74	8.46	10.43	9.71	8.19	17.67	2.64	0.17	0.06	1.18	0.81	0.87
12	31.34	0.006	0.48	1.54	2.01	6.25	7.73	7.11	5.89	11.77	2.82	0.18	0.06	1.21	0.81	0.88
14	18.64	0.005	0.36	1.10	1.45	3.97	4.59	4.03	3.20	5.38	NA	NA	0.08	1.26	0.87	0.98
16	15.49	NA	0.29	0.91	1.19	3.32	3.84	3.32	2.60	4.26	NA	NA	0.08	1.27	0.87	1.00
18	9.00	NA	0.05	0.25	0.31	1.60	2.34	2.09	1.42	1.78	NA	NA	NA	NA	NA	NA
20	7.30	NA	0.04	0.19	0.22	1.30	1.91	1.69	1.16	1.53	NA	NA	NA	NA	NA	NA
Empirical extinction coefficients (μmol m^{-2} s^{-1} cm^{-1}; 0–5 cm depth)																
Exp	−0.352	−0.418	−0.356	−0.332	−0.338	−0.351	−0.348	−0.355	−0.364	−0.392						
R^2	0.968	0.986	0.967	0.971	0.970	0.983	0.968	0.949	0.944	0.955						
Empirical extinction coefficients (μmol m^{-2} s^{-1} cm^{-1}; 0–20 cm depth)																
Exp	−0.204	−0.271	−0.214	−0.218	−0.197	−0.207	−0.202	−0.202	−0.209	−0.246						
R^2	0.920	0.950	0.955	0.956	0.960	0.941	0.929	0.936	0.953	0.962						

The potential ecological consequences of the differential spectral transmission of solar radiation through the snowpack

When considering the likely ecological effects of climate change, understanding the role of snow cover is important because the presence and depth of a snowpack has a large effect on global radiation balance.[26] Not only do the physical effects of the high albedo of snow compared with the ground, water or vegetation need to be budgeted into Earth System Models,[24,27] but the ecological interactions of the snowpack with vegetation should be incorporated into ecosystem process models considering plant production, phenology and survival.[28,29]

The insulating properties of the snowpack help to maintain the soil at a stable temperature, delaying or sometimes preventing freezing, and providing a more-stable environment for the vegetation that is encased beneath snow than that exposed above it. Fresh snow has high specific heat capacity since it holds more trapped air than denser snow which has settled over time.[10] Insulated from temperature fluctuations, plants with wintergreen leaves, or those that start to grow within the snowpack prior to snow melt in spring, require less physiological protection from cold winter temperatures and have the potential to capitalise on the sunlight they receive to photosynthesize.[30] These lower irradiances and milder temperatures within the snowpack allow leaves to have a lower light compensation point than those above the snowpack,[3] and attain a net positive carbon balance at 7 cm depth in the snowpack (receiving 10% of incident solar radiation). At low light levels, UV-A radiation has even been shown to be utilised by some plants for photosynthesis (reviewed by ref. 31) and this remains a possibility in photosynthesizing leaves at shallow depths in the snowpack.

The relative enrichment of the UV-A region, particularly at shallow depths beneath the snow surface (Fig. 2 & S5†), may be of benefit to plants and algae as a cue inducing photoprotection. The change in UV-A-to-PAR ratio in the upper centimetres of the snowpack could signal the depth of snow cover, or could even enhance *cis–syn*-cyclobutane-primidine-dimer-(CPD)-photolyase repair mechanisms, priming photosynthetic organisms for increased exposure to sunlight during snowmelt.[32]

Low-light conditions can occur because of the time of year, or be caused by shade from plants or extraneous objects, or even because of snow cover. These different scenarios will have different implications for the fitness of photosynthetic organisms and contrasting effects on spectral quality, and thus may necessitate different plant strategies for well-adapted growth and survival. Most research on plants' responses to shade has centred on shade caused by neighbouring or overtopping vegetation, but has also determined that plants can distinguish living and dead neighbours.[33] The shade avoidance syndrome (SAS) was originally considered to be triggered by the R : FR ratio and attuned by irradiance and temperature:[34] but increasingly its regulation has been found to be more intricate; with phytochromes sensing temperature,[35] as well as blue light,[36]

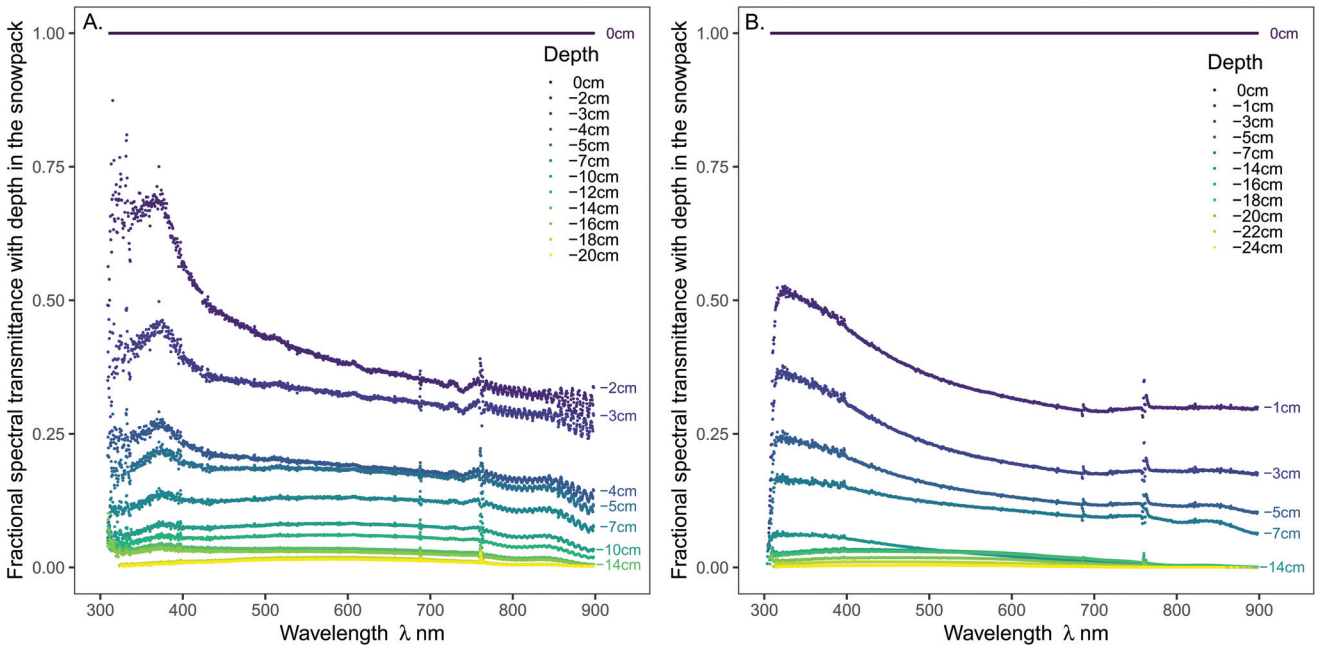

Fig. 2 Spectral transmittance as a function of depth into the snowpack, on (A) 28-02-2018 and (B) 27-01-2019. Transmittance of $y = 1$ is the normalised spectrum at the surface of the snowpack and the measured spectra are expressed as a proportion of the surface irradiance. A peak in transmittance is apparent in the 2018 profile at 365 nm in the UV-A region and another small peak at 510 nm (green region). The individual plotted points were recorded every 0.46 nm wavelength across the spectrum. The wave pattern between 750–900 nm in A is due to etaloning. Detail of the UV region is given in Fig. S3.†

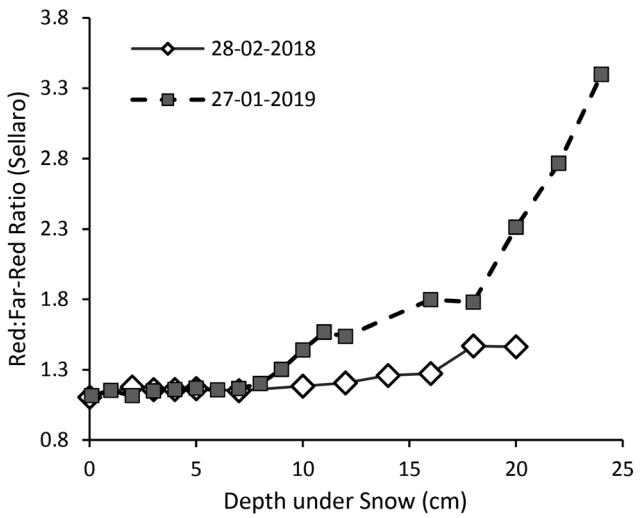

Fig. 3 The change with snow depth in the red (650–670 nm) to far-red (720–740 nm) photon ratio at the unshaded location where we measured spectral irradiance (Fig. S6†). Changes with depth in blue : green, UV-A : UV-B, and UV-A : PAR photon ratios are given in Fig. S4.†

the blue : green ratio,[12] and sunflecks[37] all contributing to the SAS. Additionally, both the total incident irradiance and its spectral composition can serve as cues for the timing of phenological events,[38] and furthermore, the proportions of UV radiation, blue and green, red and far-red light in the spectrum can function as cues affecting the allocation of resources to protection and growth.[39,40] This begs the question as to whether plants may use combinations of spectral cues to fine-tune their responses to low-light conditions, such as those within the snowpack compared with those in the shade of other plants. Just as the R : FR ratio alerts plants to the presence of living neighbouring plants rather than other objects, a spectral cue could allow plants to distinguish changes in irradiance with depth within the snowpack. For instance, in our transects the R : FR ratio increased markedly with depth under the snowpack (from 1.1 at the surface, to 1.3 (in 2018) and 1.7 (in 2019) at 16 cm depth). These enriched R : FR ratios (compared with full sun) are likely sufficient to suppress stem elongation despite the low light conditions under snow;[40] but this remains to be experimentally tested. The change in R : FR ratio with depth as the snowpack melts in spring may also be perceived by plants and could potentially serve as a regulatory cue in tandem with the UV-A-to-PAR ratio.

Plants growing above the snowpack are subject to cold temperatures and temperature fluctuations which are known to stimulate the accumulation of leaf epidermal phenolics.[41] While the leaves of evergreen and wintergreen plants protected beneath the snowpack over winter may have lower concentrations of epidermal UV-screening compounds than those above it,[30] they nevertheless maintain their UV-protection through the winter and are able to rapidly reach high photosynthetic capacity following snowmelt (Box 1). Hence, it can be expected that these plants have evolved mechanisms enabling them to pre-emptively acclimate to the drastic change in their environment that happens when the snowpack melts.

After overwintering under the snowpack plants maintain UV screening in wintergreen leaves and are able to photosynthesize efficiently in full sun following snow-melt

The benefits of snow cover for the leaves of plants preparing for the growing season are illustrated by the comparison below of *Vaccinium vitis-idaea* leaves measured directly following snow melt during March in Helsinki, Finland (2017-03-27). At midday under a mixed-forest canopy, 30 min dark-adapted leaves from plants which were snow-covered during winter had (A) a higher maximum quantum yield of photosystem II than leaves of adjacent plants exposed above the snow over winter (mini-PAM, Heinz-Walz, Germany). This difference was maintained across (B) measurements of the effective quantum yield in sun patches at midday (ΦP or F_q/F'_m), and was reflected in (C) calculations of the photosynthetic electron transfer rate ($\Phi P \times 0.5 \times \text{PAR} \times 0.84 = \text{ETR}$ μmol m^{-2} s^{-1}). Optical measurements of leaf pigments in these same leaves, made using a Dualex (Force-A, Paris, France), revealed that (D) UV-screening by epidermal flavonols was similar between the two groups of leaves, whereas (E) chlorophyll content was slightly higher in leaves that over-wintered under the snowpack but (F) epidermal anthocyanin content was slightly higher in leaves the were exposed above the snowpack over winter. Mean ± 1 SE from 6 sample locations.

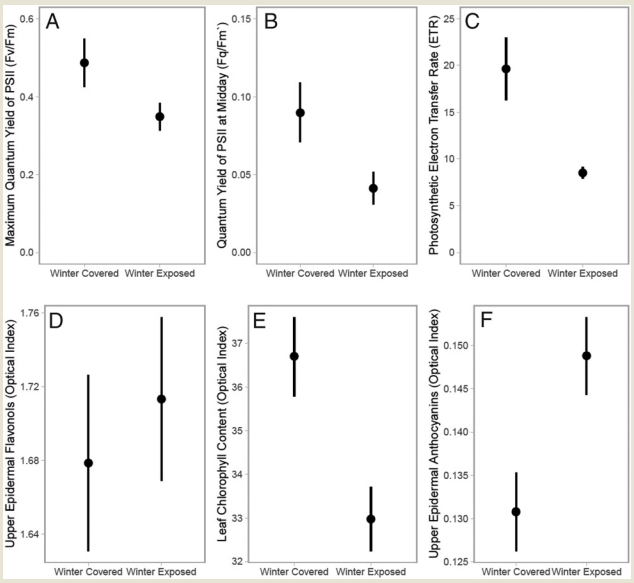

Conclusions

We successfully used a portable array spectrometer to measure *in situ* the transmission of sunlight into the snowpack down to depths of 20–24 cm, at wavelengths spanning solar UV-B and UV-A radiation, PAR, FR and near IR. The values of transmitted irradiance and extinction coefficients that we obtained largely agree both with existing models and the few available spectral measurements, in showing that about 10% of PAR reaches a depth of 7 cm in the snowpack. UV-A radiation is transmitted through snow better than longer wavelengths which are increasingly attenuated through the PAR and far red. The shift in spectral composition under snow raises the possibility that plants may detect and respond to the thickness of the snow layer covering them through perception of the altered ratio of UV-A radiation to PAR in the upper centimetres of the snowpack and/or of fine-scale spectral changes at longer wavelengths. This hypothesis is supported by our knowledge that plants and leaves emerging from the snowpack in spring acclimate quickly to the ambient environment and often show higher ecophysiological sufficiency than leaves that remained above the snowpack. Nevertheless, further research is needed to better understand how plants perceive and respond to the changing spectral irradiance under snow and whether these changes help to prime them for the onset of spring.

Description of the ESI†

Table S1: Reported transmittance of solar radiation through the snowpack in different experiments.

Table S2: Average spectral photon irradiance (μmol m^{-2} s^{-1}) given for spectral integrals, measured at 30 cm above the snow, at the snow surface (0 cm), and along a transect beneath the snow surface down to 24 cm depth (27-01-2019).

Fig. S1: Photograph of (A) the diffusor covered by 1 cm snow and (B) the measuring set-up in the field prior to measurements through the snow.

Fig. S2: Comparison of measured spectral irradiance at 30 cm above the snow and spectral irradiance modelled using libradtran (Emde *et al.* 2016) following Brelsford (2016) for 28-02-2018.

Fig. S3: Detail from Fig. 2 plotted on a $\log_{10}$ axis for the UV-region of the spectrum.

Fig. S4: Plots of the relationships of spectral integrals with snow depth on dates (A) 2018-02-28 and (B) 2019-01-27. Photosynthetically Active Radiation (PAR: 400–700 nm) is plotted on the primary axis, and unweighted UV-A (315–400 nm) and UV-B (280–315 nm) radiation on the secondary axis. At very low irradiances readings are unreliable so the UV-B line is fitted only to 12 cm depth. (C) PAR on 2018-02-28 and (D) 2019-01-27 broken down into blue (420–490 nm), green (500–570 nm) and red (620–680 nm), and far-red (700–750 nm) regions, plotted and with fitted lines (eqn 1) in their respective colours (defined according to Sellaro *et al.*, 2010) and exp in units (μmol m^{-2} s^{-1} cm^{-1}).

Fig. S5: Plots of the change ratios of spectral integrals with snow depth on each of the measurement dates. (A) Photon ratio of unweighted UV-A radiation to PAR. (B) Photon ratio of blue (420–490 nm) to green (500–570 nm) irradiance. (C) The UV-B-to-UV-A photon ratio.

Fig. S6: Hemispherical photograph taken at the location of the measurements of the snowpack. South is upper-most on the photo. The nearest vegetation was a copse of birch *c* 50 m to the north, otherwise no building or vegetation were within 100 m.

Appendix 2: solar angles and weather data (Kumpula Snow and Temperature from FMI).

Funding

Academy of Finland Fellowship (#304519 and #324555) to T. M. R. funded this research.

Conflicts of interest

There are no conflicts to declare.

Acknowledgements

Thanks to Stephan D. Flint (University of Idaho) and the University-of-Helsinki Plant-Biology Article Discussion Group for their comments on the manuscript, and to Marieke Trasser (Gregor Mendel Institute of Molecular Plant Biology in Vienna) for her participation in the experiment measuring leaf traits across snow-melt gradients in Viikki Arboretum, Helsinki.

References

1 H. L. Gorton and T. C. Vogelmann, Ultraviolet Radiation and the Snow Alga Chlamydomonas nivalis (Bauer) Wille, *Photochem. Photobiol.*, 2003, **77**, 608–615.
2 C. Körner, in *Alpine Plant Life*, Springer-Verlag, Berlin, Germany, 2003, pp. 47–62.
3 T. Saarinen, S. Rasmus, R. Lundell, O.-K. Kauppinen and H. Hänninen, Photosynthetic and phenological responses of dwarf shrubs to the depth and properties of snow, *Oikos*, 2016, **125**, 364–373.
4 W. D. Billings and L. C. Bliss, An Alpine Snowbank Environment and Its Effects on Vegetation, Plant Development, and Productivity, *Ecology*, 1959, **40**, 388–397.
5 R. W. Gerdel, Penetration of radiation into the snowpack, *Trans., Am. Geophys. Union*, 1948, **29**, 366–375.
6 H. Curl Jr., J. T. Hardy and R. Ellermeier, Spectral Absorption of Solar Radiation in Alpine Snowfields, *Ecology*, 1972, **53**, 1189–1194.
7 S. G. Richardson and F. B. Salisbury, Plant responses to the light penetrating snow, *Ecology*, 1977, **58**, 1152–1158.
8 C. S. Cockell and C. Córdoba-Jabonero, Coupling of Climate Change and Biotic UV Exposure Through Changing Snow-Ice Covers in Terrestrial Habitats¶, *Photochem. Photobiol.*, 2004, **79**, 26–31.
9 S. G. Warren, R. E. Brandt and T. C. Grenfell, Visible and near-ultraviolet absorption spectrum of ice from transmission of solar radiation into snow, *Appl. Opt.*, 2006, **45**, 5320–5335.
10 D. K. Perovich, Light reflection and transmission by a temperate snow cover, *J. Glaciol.*, 2007, **53**, 201–211.
11 J. L. France, M. D. King, M. M. Frey, J. Erbland, G. Picard, S. Preunkert, A. MacArthur and J. Savarino, Snow optical properties at Dome C (Concordia), Antarctica; implications for snow emissions and snow chemistry of reactive nitrogen, *Atmos. Chem. Phys.*, 2011, **11**, 9787–9801.
12 R. Sellaro, M. Crepy, S. A. Trupkin, E. Karayekov, A. S. Buchovsky, C. Rossi and J. J. Casal, Cryptochrome as a sensor of the blue/green ratio of natural radiation in Arabidopsis, *Plant Physiol.*, 2010, **154**, 401–409.
13 G. Casasanta and R. Garra, Towards a Generalized Beer-Lambert Law, *Fractal Fract.*, 2018, **2**, 8.
14 C. Fierz, R. L. Armstrong, Y. Durand, P. Etchevers, E. Greene, D. M. McClung, K. Nishimura, P. K. Satyawali and S. A. Sokratov, *The International Classification for Seasonal Snow on the Ground*, UNESCO-IHP, Paris, France, 2009.
15 P. J. Aphalo, Measuring solar UV-B: why is it so difficult?, in *UV4Plants Bulletin*, 2016, vol. 2016, pp. 21–28.
16 P. J. Aphalo, in *UV Radiation and Plant Life*, ed. B. Jordan, CABI International, Oxford, 2017, ch. 2, pp. 10–23.
17 P. J. Aphalo, The r4photobiology suite: Spectral irradiance, in *UV4Plants Bulletin*, 2015, vol. 2015, pp. 21–29.
18 C. Emde, R. Buras-Schnell, A. Kylling, B. Mayer, J. Gasteiger, U. Hamann, J. Kylling, B. Richter, C. Pause, T. Dowling and L. Bugliaro, The libRadtran software package for radiative transfer calculations (version 2.0.1), *Geosci. Model Dev.*, 2016, **9**, 1647–1672.
19 C. C. Brelsford, Radiative transfer theory and modelling with libRadtran, in *UV4Plants Bulletin*, 2016, vol. 2016, pp. 45–51.
20 C. F. Bohren and B. R. Barkstrom, Theory of the optical properties of snow, *J. Geophys. Res.*, 1974, **79**, 4527–4535.
21 S. Arndt, K. M. Meiners, R. Ricker, T. Krumpen, C. Katlein and M. Nicolaus, Influence of snow depth and surface flooding on light transmission through Antarctic pack ice, *J. Geophys. Res.: Oceans*, 2017, **122**, 2108–2119.
22 T. C. Grenfell, S. G. Warren and P. C. Mullen, Reflection of solar radiation by the Antarctic snow surface at ultraviolet, visible, and near-infrared wavelengths, *J. Geophys. Res.*, 1994, **99**, 18669–18684.
23 O. Järvinen and M. Leppäranta, Solar radiation transfer in the surface snow layer in Dronning Maud Land, Antarctica, *Polar Sci.*, 2013, **7**, 1–17.
24 P. Räisänen, R. Makkonen, A. Kirkevåg and J. B. Debernard, Effects of snow grain shape on climate simulations: sensitivity tests with the Norwegian Earth System Model, *Cryosphere*, 2017, **11**, 2919–2942.
25 T. U. Kaempfer, M. A. Hopkins and D. K. Perovich, A three-dimensional microstructure-based photon-tracking model of radiative transfer in snow, *J. Geophys. Res.*, 2007, **112**, 14.

26 S. Rasmus, D. Gustafsson, R. Lundell and T. Saarinen, Observations and snow model simulations of winter energy balance terms within and between different coniferous forests in Southern Boreal Finland, *Hydrol. Res.*, 2015, **47.1**, 201–217.

27 S. D. Wullschleger, H. E. Epstein, E. O. Box, E. S. Euskirchen, S. Goswami, C. M. Iversen, J. Kattge, R. J. Norby, P. M. van Bodegom and X. Xu, Plant functional types in Earth system models: past experiences and future directions for application of dynamic vegetation models in high-latitude ecosystems, *Ann. Bot.*, 2014, **114**, 1–16.

28 A. J. Leffler and J. M. Welker, Long-term increases in snow pack elevate leaf N and photosynthesis in Salix arctica: responses to a snow fence experiment in the High Arctic of NW Greenland, *Environ. Res. Lett.*, 2013, **8**, 025023.

29 P. Niittynen, R. K. Heikkinen and M. Luoto, Snow cover is a neglected driver of Arctic biodiversity loss, *Nat. Clim. Change*, 2018, **8**, 997–1001.

30 T. Solanki, P. J. Aphalo, S. Neimane, S. M. Hartikainen, M. Pieriste, A. Shapiguzov, A. Porcar-Castell, J. Atherton, A. Heikkila and T. M. Robson, UV-screening and spring-time recovery of photosynthetic capacity in leaves of Vaccinium vitis-idaea above and below the snow pack, *Plant Physiol. Biochem.*, 2019, **134**, 40–52.

31 D. Verdaguer, M. A. Jansen, L. Llorens, L. O. Morales and S. Neugart, UV-A radiation effects on higher plants: Exploring the known unknown, *Plant Sci.*, 2017, **255**, 72–81.

32 K. Brettel and M. Byrdin, Reaction mechanisms of DNA photolyase, *Curr. Opin. Struct. Biol.*, 2010, **20**, 693–701.

33 C. L. Ballare, R. A. Sanchez, A. L. Scopel, J. J. Casal and C. M. Ghersa, Early detection of neighbour plants by phytochrome perception of spectral changes in reflected sunlight, *Plant, Cell Environ.*, 1987, **10**, 551–557.

34 J. J. Casal and J. I. Questa, Light and temperature cues: multitasking receptors and transcriptional integrators, *New Phytol.*, 2018, **217**, 1029–1034.

35 M. Legris, C. Klose, E. S. Burgie, C. C. Rojas, M. Neme, A. Hiltbrunner, P. A. Wigge, E. Schafer, R. D. Vierstra and J. J. Casal, Phytochrome B integrates light and temperature signals in Arabidopsis, *Science*, 2016, **354**, 897–900.

36 D. H. Keuskamp, R. Sasidharan, I. Vos, A. J. Peeters, L. A. Voesenek and R. Pierik, Blue-light-mediated shade avoidance requires combined auxin and brassinosteroid action in Arabidopsis seedlings, *Plant J.*, 2011, **67**, 208–217.

37 V. Moriconi, M. Binkert, C. Costigliolo, R. Sellaro, R. Ulm and J. J. Casal, Perception of Sunflecks by the UV-B Photoreceptor UV RESISTANCE LOCUS8, *Plant Physiol.*, 2018, **177**, 75–81.

38 C. C. Brelsford, L. Nybaken, T. K. Kotilainen and T. M. Robson, The influence of spectral composition on spring and autumn phenology in trees, *Tree Physiol.*, 2019, **tpz026**, 1–26, DOI: 10.1093/treephys/tpz026.

39 S. Hayes, C. N. Velanis, G. I. Jenkins and K. A. Franklin, UV-B detected by the UVR8 photoreceptor antagonizes auxin signaling and plant shade avoidance, *Proc. Natl. Acad. Sci. U. S. A.*, 2014, **111**, 11894–11899.

40 C. L. Ballare and R. Pierik, The shade-avoidance syndrome: multiple signals and ecological consequences, *Plant, Cell Environ.*, 2017, **40**, 2530–2543.

41 W. Bilger, M. Rolland and L. Nybakken, UV screening in higher plants induced by low temperature in the absence of UV-B radiation, *Photochem. Photobiol. Sci.*, 2007, **6**, 190–195.